Article:
Robinson, Matthew S., Lane, Paul D. and Wann, Derek A. orcid.org/0000-0002-5495-274X (2016) Simulations of the temporal and spatial resolution for a compact time-resolved electron diffractometer. Journal of Physics B: Atomic, Molecular and Optical Physics. 034003. ISSN 1361-6455

https://doi.org/10.1088/0953-4075/49/3/034003

Simulations of the temporal and spatial resolution for a compact time-resolved electron diffractometer

Matthew S. Robinson,[1,2] Paul D. Lane[1,3] and Derek A. Wann[1]

[1] Department of Chemistry, University of York, Heslington, York, YO10 5DD, UK.

[2] Present address: Department of Physics and Astronomy, University of Nebraska–Lincoln, Theodore Jorgensen Hall, 855 N 16th Street Lincoln, NE 68588-0299, USA.

[3] Present address: School of Engineering and Physical Sciences, Heriot-Watt University, Edinburgh, EH14 4AS, UK

Abstract

A novel compact electron gun for use in time-resolved gas electron diffraction experiments has recently been designed and commissioned. In this paper we present and discuss the extensive simulations that were performed to underpin the design in terms of the spatial and temporal qualities of the pulsed electron beam created by the ionisation of a gold photocathode using a femtosecond laser. The response of the electron pulses to a solenoid lens used to focus the electron beam has also been studied. The simulated results show that focusing the electron beam affects the overall spatial and temporal resolution of the experiment in a variety of ways, and that factors that improve the resolution of one parameter can often have a negative effect on the other. A balance must, therefore, be achieved between spatial and temporal resolution. The optimal experimental time resolution for the apparatus is predicted to be 416 fs for studies of gas-phase species, while the predicted spatial resolution of better than 2 nm^{-1} compares well with traditional time-averaged electron diffraction set-ups.

Keywords: electron diffraction, time-resolved electron diffraction, spatial resolution, temporal resolution

1. Introduction

Since the founding work of Davisson and Germer in the 1920s [1] many electron diffraction studies have been performed using continuous beams of electrons to collect time-averaged structural information for countless gaseous and solid-state molecules. Because of the nature of these continuous electron beams, most electron diffraction experiments have been performed for static systems averaged over all populated vibrational states. While this has proved to be a useful tool in determining molecular structures, which in turn have provided great insights into molecular function, studying the dynamics of structural changes has the potential to yield even more useful information. More recently, electron diffraction has moved into the time-resolved domain, with developments ongoing to allow changes in molecular structure to be studied in real time [2]. In instrumentation terms this has meant replacing the continuous electron beam with a pulsed beam to capture near-instantaneous images. Early time-resolved electron diffractometers (TREDs) used rapidly switching electric fields to produce stroboscopic electron beams [3] to study the dynamics of molecular systems on the microsecond timescale. However, most modern TRED apparatus make use of ultrafast electron pulses created by the ionisation of a photocathode using a femtosecond laser source [4], and are accelerated across potentials ranging from 30 to 200 keV; these are typically used to study photoinduced changes in molecular structure on the pico- and femtosecond timescales [5–8].

Elsewhere, time-resolved diffraction has been achieved using ultrafast X-ray diffractometers [9,10], though such experiments (with a few exceptions) [11] require the use of large and expensive facilities, such as synchrotrons and free-electron lasers, to produce X-rays of a suitable duration and brightness. Meanwhile, the use of MeV electrons for diffraction has been demonstrated, although such large accelerating potentials generally require accelerator technology [12–15].

It is the relative simplicity in how electron pulses are created in keV TRED experiments that has allowed for cost-effective table-top apparatus to be designed and built. Many variations in the basic idea have been published, from the simple compact electron gun [5,16–18], to devices that use radio-frequency (RF) cavities [19–21], or reflectrons [22] to compress pulses in order to observe even faster dynamics. Other apparatus make use of long electron pulses and streak camera technology [23] to study molecular dynamics in a single shot, rather than as a series of time-separated experiments.

Recently, we presented a new compact electron gun apparatus for TRED experiments, in which we showed experimentally that with a solenoid lens it was possible to focus an electron beam at the detector increasing the sharpness of the rings observed from the diffraction of a thin polycrystalline Pt sample [18]. For a number of apparatus reported in the literature the magnetic lens is placed in a fixed position on, or very close to, the anode and is simply used to obtain the best focus of the electron beam upon the detector [24,25]. This may not, however, be the optimal set-up for the experiment as whole.

The work presented here documents a series of simulations used to investigate how both the position and power of the magnetic lens within a compact electron gun can affect the properties of an electron beam. We show that with careful selection of these lens properties one is able to optimise a beam that not only has a small spot size at the detector, to give a clear diffraction pattern, but also a small spot size at the sample to improve the experimental temporal resolution.

2. Experimental considerations

Much of the early work on TRED was performed by Zewail [5,26,27] the Nobel Prize winner for the foundations of femtochemistry [28] and his co-workers, and so it is of no surprise that most TRED experiments follow the pump-probe methodology used in these experiments.

This usually involves exciting a molecule from its ground vibrational and electronic state into a higher electronic state using a suitable pump, which for most experiments will come from a laser source. The response of the molecule to this pump is then monitored using an electron probe pulse. By varying the arrival time of the probe with respect to the pump, the dynamical behaviour of the molecule can be deduced.

The information that can be discerned from a TRED experiment depends on the resolution of the experiment, which in turn depends on the properties of the pump and probe beams. Work by Zewail *et al.* highlighted the velocity mismatch problem [29] and showed that the overall time resolution of an experiment is dependent on factors such as the width, duration, and group velocity of the probing electron pulse, as well as the relative angle between the pump and probe beams at the sample. Generally, the best experimental time resolution is observed when the pump, probe, and molecular beams (or solid sample) are as narrow as possible, with short pulse durations of the pump/probe beams. Therefore, to obtain the best experimental time resolution the properties of both laser and electron beams must be carefully controlled. Of the two, the laser beam is generally the better understood and more stable, whilst the electron probe can be more variable. Its behaviour is dependent on factors such as the number and initial kinetic energy distribution of the electrons, the accelerating potential applied, and the ever present space-charge repulsion [30,31]. How these affect the pulse duration is already well understood [25,30], with Siwick *et al.* showing that a 30 keV pulse containing 10^4 electrons with initial duration of 50 fs will have expanded to 6.5 ps by the time it has propagated for 4 ns [30]. This is the idea behind the compact electron gun; using short electron source-to-sample distances to minimise this temporal expansion of a pulse. However, as previously mentioned, the transverse width of the electron beam not only affects the final diffraction pattern but plays a significant role in the total time resolution of a TRED experiment [29], as will become more apparent later on.

Similarly the quality of structural information obtained from time-resolved diffraction experiments is dependent on a number of factors, including beam size, pulse duration, temporal and spatial coherence lengths, the electron dose, and the scattering angle considered.

For the work presented here we make the assumption that the electron dose is varied only by recording more shots rather than by increasing the number of electrons per shot. We assume that the experiment is set up such that data can be recorded over a scattering range that is sufficient to determine the structure of small molecules (< ~50 atoms) at a single sample-to-detector distance – which, based on a survey of the literature, a range of $20 \leq s \leq 200$ nm^{-1} is sufficient [32].

Spatial (transverse) coherence is an important factor in determining the quality of electron beams for diffraction experiments as well as electron microscopy [33,34], and becomes a more significant factor as molecules of interest become larger *e.g.* biological molecules. High coherence within the electron beam can be obtained by careful selection of the beam source and the conditions under which the beam is emitted. For example, both nanotips [34] and ultracold gases [35] can offer a more coherent electron beam than that produced from a thin-film photocathode. However, these higher coherent sources are generally not as robust as the more commonly used thin-film photocathode, with lower damage thresholds [36] or reduced firing rates [34]. The transverse coherence for electron beams in the 60-100 keV range of ~150-200 μm diameter has been estimated [20,25] to be ~2-3 nm. For single electron sources, Baum [34] notes that although converging or diverging beams are often used in diffraction [25,37], the global degree of coherence is conserved and so the ratio of coherence length to beam diameter remains constant. Yet, in the case of high-density electron beams, space-charge heating, or distortion of the phase space by space-charge effects, can limit this ratio between the transverse coherence length and the beam diameter [38]. However, for the work

considered here sufficiently few electrons are used per pulse that no distortion of the phase-space is observed within the proximity of high-electron-density regions (*i.e.* the electron source or the focus of the electron beam produced by the magnetic lens). Throughout all simulations presented we observe a linear correlation between position and momentum indicating that the space-charge induced thermal effects are minimal, and so therefore can assume that the global coherence of the experiment is unaffected [39], with similar conclusions being drawn by Gahlmann *et al.* [25]. It should be noted, however, that slightly different initial conditions (*i.e.* shorter initial pulse durations, larger acceleration potentials) may result in different growth mechanisms occurring [25,38,39].

Given these observations, in this work we shall consider the beam size as an indicator of spatial beam quality. As noted by Baum [34], the coherence time and longitudinal coherence length are "almost irrelevant for diffraction" except in cases where electron-pulse durations are compressed, or where energies are measured in the experiment. As this work considers a compact electron gun design, we deem it unnecessary to consider either of these factors when considering the quality of the electron beam. Finally, the size of the electron beam at the detector also plays a role in the resolution of a diffraction pattern, with the distinct diffraction rings observed in gas-phase and polycrystalline experiments becoming blurred when wider beams are used [25].

3. Experimental section

3.1. Simulation set-up

The simulations presented here were performed using General Particle Tracer (GPT) [40,41] and space-charge effects were modelled using the spacecharge3D algorithm in GPT. Most parameters were chosen to match the compact electron gun apparatus in York [18]; however, a generic model of the magnetic lens has been used due to the numerous ways one could

design it to produce the same magnetic fields. A schematic of the set-up is shown in Figure 1. As other studies have already shown that the properties of an electron beam vary with the number of electrons and several other initial conditions [17,25,30], this work focuses on how the properties of the beam change as a function of factors common to a compact electron gun, such as the distance, *P*, between the photocathode and anode, the distance, *L*, between the anode and the lens, the magnetic field strength of the lens, and the size of the aperture, *a*, in the anode.

In the simulations a 250 nm laser pulse with a duration of 120 fs and a 200 μm FWHM diameter produces an electron pulse from a gold photocathode with very similar initial properties to the laser [42]. The electron pulse is modelled to have a Gaussian spread of kinetic energies centred on 0.7 eV and with an FWHM value of 0.6 eV, as based on the experimentally determined values for a gold thin film [31] similar to the one used in the apparatus described in ref. 18. Other studies have already examined how kinetic energy distributions and initial beam sizes affect the properties of a pulsed electron beam [17,25]. The initial space-charge effects lead to the strong growth of the transverse and longitudinal phase space which are sensitive to these initial parameters, and these effects have been studied in detail elsewhere [38,39]. The work here considers an electron source with a longer pulse duration and with fewer electrons per pulse in which no significant thermal space-charge effects were observed.

Figure 1. A schematic diagram of the TRED set-up.

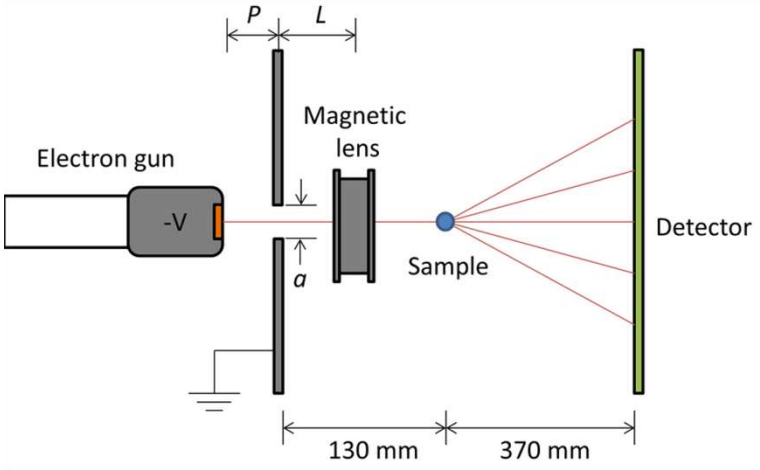

The number of electrons per pulse has a significant effect on the electron pulse duration and, hence, the overall temporal resolution. In this work we have modelled 10^4 electrons per pulse as it has been shown that the rate of expansion of the pulse in the temporal frame is not too large [30]. These 10^4 electrons are described by 10^3 macroparticles, each representing ten electrons. This number of macroparticles was found to provide similar results on test measurements to those with 10^4 macroparticles but was much less computationally expensive; this approach has also been used in other similar studies [17]. After creation, the electrons are accelerated across a potential, V, of up to 100 kV towards a grounded anode into which apertures of various sizes can be inserted.

The field-free region is the major part of the chamber and is bounded by the anode of the electron gun at one end and the detector at the other, and houses the magnetic lens and sample. The magnetic lens is modelled as a single solenoid, 10 mm in diameter, acting over a length of 20 mm, allowing for a field of up to 126 mT to be applied. Whilst this model is loosely based on the lens seen in ref. 18 (which has 1000 turns and allows a current of up to 2 A), in this work we have kept the lens model simple so as to remain generic; the field strengths quoted here can be obtained using numerous combinations of solenoid diameter, length and quality of winding.

The sample, which for this study is taken to be a gas-phase molecular beam (although the principles apply equally to all samples), is positioned 130 mm from the anode with the detector positioned 370 mm beyond the sample.

4. Results and discussion

Due to the Gaussian nature of the laser used to produce electrons, the temporal dimension of the electron beam is treated in a similar fashion and its size is given as its FWHM. On the other hand, although the transverse dimension of the electron pulse is initially described using a Gaussian profile, after having the outermost electrons removed as it passes through the aperture in the anode, and due to the ultrashort nature of the pulse, the beam can be approximated to be a flat disc. Because of this, we describe the spot size of the beam at points throughout its propagation in terms of its root-mean-square (rms) radius. It is worth noting that the beam waist of the focus does not necessarily occur at the sample position. We are interested in the properties of the electron beam where it interacts with the sample; as the thermal space-charge effects are negligible we assume that the coherence length remains proportional to the beam size at positions away from the beam waist. As necessitated by the velocity mismatch equations [29], a FWHM equivalent is given for the transverse size of the pulse for chosen values when discussing the overall experimental time resolution.

4.1. Electron pulse properties

4.1.1. Without magnetic lens

So as to have a comparative control, the natural properties of the electron beam were simulated under various initial conditions, including different accelerating potentials (45, 65 and 100 kV), photocathode-to-anode distances (10 and 15 mm) and aperture sizes (150 and 400 μm) without the presence of a magnetic lens.

The number of electrons predicted to pass through a given aperture and travel to the sample and detector is dependent on the size of the apertures used, although, as shown in Table 1, there seems to be little variation with respect to the photocathode-to-anode distance and acceleration potential used. For the smaller 150 μm aperture only 24% of the original 10^4 electrons pass through, while with the larger 400 μm aperture this increases significantly, to around 86%. As more electrons reach the sample and detector with the larger aperture, collection of diffraction data will theoretically take less time.

Table 1. Summary of the pulse duration and transverse beam size at key points throughout the apparatus for different electron gun conditions.

photocathode-to-anode distance / mm	aperture size / μm	acceleration potential / kV	% of electron beam passing through aperture	pulse duration at sample / fs	RMS beam radius at sample / mm	RMS beam radius at detector / mm
10	150	45	23.8	938	0.24	0.81
		65	23.9	630	0.24	0.80
		100	24.1	398	0.24	0.80
	400	45	86.0	923	0.54	1.75
		65	86.2	621	0.54	1.75
		100	86.4	392	0.54	1.76
15	150	45	23.3	1295	0.19	0.60
		65	23.8	886	0.19	0.58
		100	23.9	562	0.18	0.57
	400	45	86.0	1303	0.41	1.27
		65	86.4	881	0.41	1.25
		100	86.8	558	0.41	1.25

Figure 2. Graphs showing the predicted a) pulse duration and b) RMS beam radius of an electron pulse, initially containing 10^4 electrons passing through apertures of various sizes, for different acceleration potentials and for 10 mm photocathode-to-anode distance electron gun.

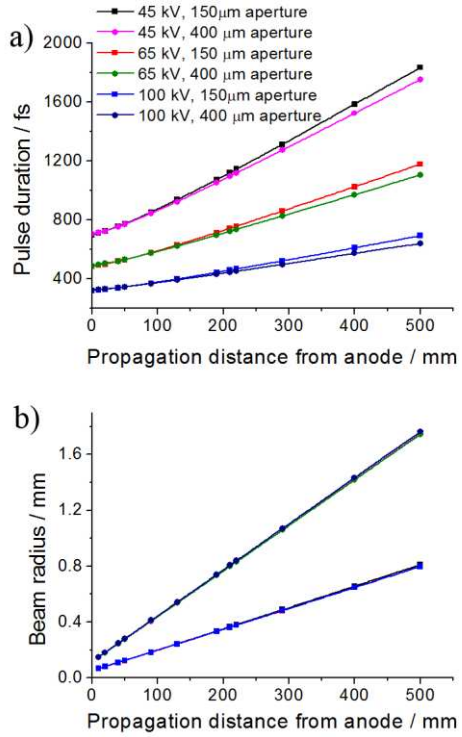

The graphs shown in Figure 2 indicate how the duration and the transverse beam size of the electron pulse evolves as it propagates through the apparatus under different initial conditions for an electron gun with a 10 mm photocathode-to-anode electron gun (equivalent results for a 15 mm photocathode-to-anode electron gun can be found in Figure S1). Key values relating to pulse duration and beam size throughout the propagation of a pulse, using simulations for both the 10 and 15 mm photocathode-to-anode distance, are also summarised in Table 1. As is the basic principle of the compact electron gun, shorter pulse durations are observed at all points throughout the flight of the electrons when using higher acceleration potentials and shorter photocathode-to-anode distances. However, it appears that the observed pulse duration is independent of the size of aperture used, due to the aperture only removing the outer electrons from the pulse, keeping the core electron density the same.

The results also show that the transverse radius of the electron pulses do not vary appreciably with the acceleration potential of the electron gun, but is strongly dependent on the aperture size, with a larger transverse radius observed with the larger aperture. This is likely to be related to the fact that the transverse kinetic energy of the electrons is negligible compared to that of the direction of propagation, and the width is more dependent on the shape of the electric field between the anode and cathode of the electron gun.

The simulations show that whilst an increased pulse duration is observed with the larger photocathode-to-anode distance, the radius of the electron beam is narrower compared to its shorter photocathode-to-anode counterpart. As the simulations show that there is no detrimental effect in the number of electrons that pass through the aperture for different photocathode-to-anode distances, the ability to vary the photocathode-to-anode distance could allow experimentalists to trade temporal resolution for spatial resolution in order to closely examine different features of a diffraction pattern.

By looking at the electron beam sizes in Table 1 one can see that the large beam sizes would make extracting well-resolved diffraction data difficult for the range of potentials typically used in these types of experiments. Therefore, it would be desirable to use a magnetic lens to compress the electron pulse in the transverse direction to improve spatial resolution. However, how the magnetic lens affects the other properties of the pulse and the experiment as a whole must be investigated.

4.1.2. With magnetic lens

The effect on the properties of the electron beam as it is focused by a magnetic lens positioned at various points throughout the propagation of the beam for a series of different magnetic field strengths was investigated by placing the centre of the lens at 10 mm intervals between the anode of the electron gun and the sample position (*i.e.* between 10 mm and 120

mm from the anode of the electron gun), whilst a field strength between 0 and 126 mT (in intervals of 12.6 mT) was simulated at each of these positions.

4.2. Beam size

Details of all the calculations carried out for this study can be found in full in the Supporting Information, in Tables S1–S132; however, in the interest of space, in this section we will focus on those calculations that will give appreciably better resolved diffraction data. Therefore, we will forego discussion of simulations that either a) under-focus the electron beam, or b) over-focus the electron beam.

Situation a) arises where the magnetic lens field strength is too low (generally, $B < 25.2$ mT) to affect the overall electron beam width appreciably. Situation b) occurs where the magnetic lens field strength is large enough (generally $B > 88.2$ mT) to cause over-focussing of the electron beam, creating beams that are larger than 10 mm in diameter at the detector.

Figure 3. Variation in the beam radius of a 45 keV electron pulse from an electron gun with a 15 mm photocathode-to-anode distance under the following initial conditions: A) 150 µm aperture, no magnetic lens; B) 400 µm, no magnetic lens; C) 150 µm aperture, magnetic lens at 120 mm (from anode), 37.8 mT; D) 400 µm aperture, lens at 120 mm, 37.8 mT; E) 400 µm aperture, lens at 10 mm, 37.8 mT; F) 150 µm aperture, lens at 80 mm, 37.8 mT.

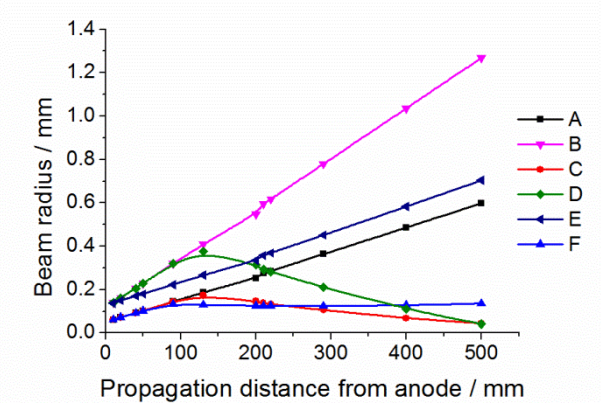

Figure 3 shows the predicted electron beam radius from simulations of a 45 keV electron gun with a 15 mm photocathode-to-anode distance for various initial and magnetic lens conditions. Cases A and B show the how the radius of the electron beam naturally expands as

it propagates through the apparatus for apertures of 150 and 400 μm used in the anode of the electron gun, respectively. Cases C and D introduce a magnetic lens for the beams seen in A and B, respectively, and highlight the fact that the best beam focus at the detector can be obtained when the lens is positioned late in the propagation of the beam. In case C, the electron beam has an rms radius of 0.172 mm at the sample, whilst case D has an approximate 0.38 mm beam radius at the same point. Coincidently, both beams have a radius of around 0.04 mm at the detector, small enough for the experiment to be considered to have high spatial resolution. This optimal focus upon the detector is achieved with the lens in this position due to two related points. The first comes from the fact that the distance between the lens and the detector is relatively short, giving less time for the electron beam to recover from the focussing effect of the lens, restricting its potential to expand again. The second is due to the lower electron density within the pulse after already having time to expand in both the temporal and spatial dimensions in the propagation up to the lens, which in turn makes it easier to compress. One can see that by placing the lens nearer to the anode (as in case E), where the beam is still narrow, it is more difficult to compress the beam due to an increased charge density at the point of focussing.

Whilst we have shown the general conditions necessary to obtain the narrowest beam at the detector, this will not necessarily produce the optimal beam size at the sample. In case F, the set-up has been kept the same as in C, but the magnetic lens has been moved back to about 80 mm from the anode. In doing this, it has been possible to create a narrow and relatively collimated electron beam throughout the apparatus, the size of which is 0.136 mm in radius at the detector (just over three times larger than the ‘optimal’ focus) but is now almost a third smaller (at 130 μm) at the sample position, than was seen with the lens 40 mm forward from this position.

With the added effect that a narrower beam at the sample gives an increased time resolution for the experiment as a whole, this collimated electron beam may be the compromise needed to observe certain events with high spatial resolution. By fine tuning the position and current of the lens to values that are between the points analysed in this paper it may be possible to obtain a more optimally collimated electron beam. Similar results were observed for other electron gun energies, and initial conditions, full details of which can be found in the Supporting Information.

4.3. Pulse duration

As a pulse is compressed by the magnetic lens in the transverse plane, its charge density will increase, causing it to stretch in the temporal direction. How much the duration is affected is obviously dependent on the focusing properties of the magnetic lens, and how far the pulse has to propagate after focusing has begun. Figure 4 shows how the duration of a pulse, at the sample position, produced from an electron gun with a 400 μm aperture and 15 mm photocathode distance with various accelerating potentials varies for different field strengths and positions from the anode for the magnetic lens.

Figure 4. Variation in the duration at the sample position of a) 45 keV and b) 100 keV electron pulses passing through a 400 μm aperture in the anode from a 15 mm photocathode-to-anode distance electron gun, as the field strength and position of the magnetic lens (with respect to the anode) is adjusted.

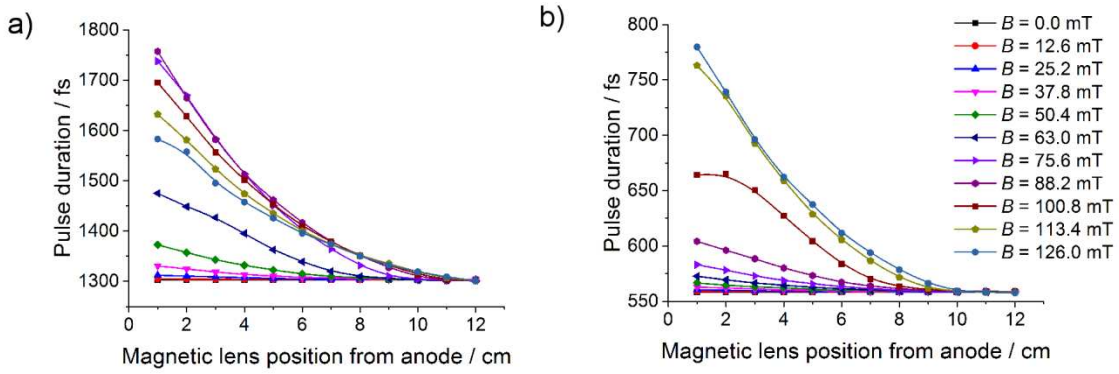

Immediately one can see that the magnetic lens has a more adverse effect on the duration of the electron pulse when it is placed far away from the sample (*i.e.* closer to the anode), and to a point, the duration worsens as the field strength of the lens increases. This stretching arises due to a combination of the increased charge density within the pulse caused by its compression, and the distance that the pulse has to travel to the sample. As would be expected, the rate of pulse expansion is much less for larger accelerating potentials, as it takes less time for the electrons to reach the sample.

For all magnetic field strengths, as the lens is brought towards the sample, the rate at which the electron beam expands in the temporal direction decreases as there is less time for the pulse to stretch, and converges to the duration seen with the natural electron pulse. However, even before the lens is positioned this close to the sample, for field strengths that do not cause an over-focussing of the beam, the increase in the pulse duration is almost negligible.

The pulse duration of the electron beam at the sample position has been calculated for other electron gun and magnetic lens set-ups, and can be found in the Supporting Information Tables S133–S144.

4.4. Velocity mismatch

Throughout this we have suggested that certain magnetic lens focusing conditions may improve the overall experimental time resolution and, in Table 2, examples of the expected spatial and temporal resolution for different electron gun and magnetic lens conditions have been presented. In predicting the experimental resolution we have used the velocity mismatch equations set out by Zewail *et al.* [29], and have chosen to deal with the simplest laser-electron beam crossing where they meet at right angles to one another at the sample. In terms of the width of the laser and molecular beams, initially these have been set to match the width of the natural electron beam, so as to observe the largest amount of diffraction possible. This assumes that the three beams cross perfectly and that the laser acts on the whole molecular

beam. We then look to see how the magnetic lens affects the overall resolution as the sizes of the molecular and laser beams are re-optimised to match the size of the electron beam at the sample. With careful planning, any of the experimental geometries presented can be obtained. As previously mentioned, the velocity mismatch equations require the width of the electron beam to be represented by its FWHM. Due to the aperture removing the outer electrons of the beam, the FWHM presented here will be more accurate for the electron beam that passes through the larger aperture than the smaller aperture as it remains more Gaussian in shape.

To return to the 45 kV, 150 μm aperture, 15 mm photocathode-to-anode distance electron gun that was discussed in Figure 3, the predicted pulse duration at the sample without the presence of a magnetic lens is 1,295 fs. Taking into account velocity mismatch, the expected time resolution for the experiment is 2,192 fs, with a 600 μm beam radius at the detector. In the case where the magnetic lens is used to obtain the best beam radius of 40 μm on the detector, improves the resolution to 2,067 fs. Yet in the case of the collimated electron beam, which has a narrower electron beam at the sample, but a larger a beam radius at the detector of 136 μm, the experimental time resolution is 1,825 fs. The resolution of this experiment is 17% better than that which uses the natural electron beam alone.

At higher acceleration potentials, the effect of the magnetic lens is even greater. For a 100 kV, 150 μm aperture electron gun with a 10 mm photocathode-to-anode distance, the pulse duration at the sample is 398 fs, and produces an overall time resolution of 1,761 fs for the natural beam. However, when an optimal focus of the beam radius at the detector of 10 μm is achieved, the time resolution improves to 1,296 fs. Furthermore, for the collimated electron beam, which has a radius of 100 μm at the detector, the time resolution improves to 841 fs – an improvement of 52% on the unoptimised set-up.

Additionally, if one was to adjust the incident angle between the laser and electron beam to 57°, the overall experimental resolution increases again to 667 fs. However, one should note

that this could be improved if lasers with appropriately tilted wavefronts (of the same angle, 57°) are used, giving a potential time resolution of 416 fs [43].

One can clearly see that, although there is a loss in the spatial resolution of the experiment, by using the collimated electron beam and not the best focus on the detector the temporal resolution can be dramatically improved. The experimental time resolution for other electron gun and magnetic lens conditions have been calculated, and can be found in the Supporting Information in Tables S145–S150.

Table 2. Predicted experimental outcomes and resolution for selected electron gun and magnetic lens conditions.

acceleration potential / kV	photocathode-to-anode distance / mm	aperture size / μm	lens position / mm	lens field strength / mT	focus type	electron beam rms radius at sample / mm	equivalent FWHM beam size / mm	electron pulse duration / fs	laser and sample width / mm	time-resolution / fs	electron beam rms radius at detector / mm
45	15	150	–	0.0	Natural	0.187	0.263	1295	0.275	2192	0.600
			120	37.8	Optimal detector focus	0.172	0.241	1297	0.250	2067	0.040
			80	37.8	Collimated	0.130	0.181	1296	0.200	1825	0.136
100	10	150	–	0.0	Natural	0.243	0.334	398	0.350	1761	0.800
			100	63.0	Optimal detector focus	0.182	0.248	398	0.250	1296	0.010
			40	75.6	Collimated	0.100	0.137	405	0.150	841	0.100

5. Conclusions

The simulations presented here have shown how a pulsed electron beam in a compact electron gun is affected by the position and power of a magnetic lens in terms of both its temporal duration and transverse spatial size, for various initial electron gun conditions. The simulations show that simply focusing the beam onto the detector is not necessarily the best solution. Overall, a poorer spatial and temporal resolution is obtained with the magnetic lens closer to the source of the electrons; with careful manipulation of the lens to other positions, one can achieve either better spatial or temporal resolution from an experiment. With these ideas in mind, these results should help experimentalists obtain the desired information and resolution from their own time-resolved electron diffraction experiments.

Supporting Information

Detailed results relating to the calculations discussed within this paper can be found in the accompanying Supporting Information. Figure S1 contains graphs that detail how the temporal and spatial properties of an electron pulse containing 10^4 electrons various as it propagates through the apparatus under different electron gun initial conditions. Tables S1–S132 contain details of how the electron beam radius varies under different initial conditions for all the calculations carried out for this study. Tables S133–S144 contain the pulse duration of the electron beam at the sample position calculated for electron gun and magnetic lens set-ups other than those described in the paper. Tables S145–S150 contain the experimental time resolution for alternative electron gun and magnetic lens conditions.

Acknowledgements

The authors are grateful to the EPSRC for funding (EP/I004122), and P.D.L. would like to

thank the University of Edinburgh Innovation Initiative Fund for software provision. We acknowledge the University of Edinburgh and the University of York for providing facilities. Finally we thank Stuart Young and Conor Rankine (University of York), and Prof. Dwayne Miller and Dr. Stuart Hayes (MPSD Hamburg) for useful discussions. All data supporting this study are provided either in the results section of this paper or as supplementary information accompanying this paper.

References

[1] Mark H and Wierl R 1928 *Naturwissenschaften* **18** 778

[2] Gao M, Lu C, Jean-Ruel H, Liu L C, Marx A, Onda K, Koshihara S-Y. Nakano Y, Shao X, Hiramatsu T *et al.* 2013 *Nature* **496** 343

[3] Ischenko A A, Golubkov V V, Spiridonov V P, Zgurskii A V, Akhmanov A S, Vabischevich M G and Bagratashvili V N 1983 *Appl. Phys. B* **32** 161

[4] Ewbank J D, Faust W L, Luo J Y, English J T, Monts D L, Paul D W, Dou Q and Schäfer L 1992 *Rev. Sci. Instrum.* **63** 3352

[5] Williamson J C, Cao J, Ihee H, Frey H and Zewail A H 1997 *Nature* **386** 159

[6] Sciaini G, Harb M, Kruglik S G, Payer T, Hebeisen C T, zu Heringdorf F-J M, Yamaguchi M, Horn-von Hoegen M, Ernstorfer R and Miller R J D 2009 *Nature* **458** 56

[7] Jean-Ruel H, Gao M, Kochman M A, Lu C, Liu L C, Cooney R R, Morrison C A and Miller R J D 2013 *J. Phys. Chem. B* **117** 15894

[8] Hensley C, Yang J and Centurion M 2012 *Phys. Rev. Lett.* **109** 133202

[9] Schotte F, Lim M, Jackson T A, Smirnov A V, Soman J, Olson J S, Phillips Jr G N, Wulff M and Anfinrud P A 2003 *Science* **300** 1944

[10] Reusch T, Mai D, Osterhoff M, Khakhulin D, Wulff M and Salditt T 2013 *Phys. Rev. Lett.* **111** 268101

[11] Elsaesser T and Woerner M 2010 *Acta Crystallogr. A* **66** 168

[12] Hastings J B, Rudakov F M, Dowell D H, Schmerge J F, Cardoza J D, Castro J M, Gierman S M, Loos H and Weber P M 2006 *Appl. Phys. Lett.* **89** 184109

[13] Musumeci P, Moody J T, Scoby C M, Gutierrez M S and Westfall M 2010 *Appl. Phys. Lett.* **97** 063502

[14] Li R, Huang W, Du Y, Yan L, Du Q, Shi J, Hua J, Chen H, Du T, Xu H, *et al.* 2010 *Rev. Sci. Instrum.* **81** 036110

[15] Weathersby S P, Brown G, Centurion M, Chase T F, Coffee R, Corbett J, Eichner J P, Frisch J C, Fry A R, Gühr M, Hartmann N, Hast C, Hettel R, Jobe R K, Jongewaard E N, Lewandowski J R, Li R K, Lindenberg A M, Makasyuk I, May J E, McCormick D, Nguyen M N, Reid A H, Shen X, Sokolowski-Tinten K, Vecchione T, Vetter S L, Wu J, Yang J, Dürr H A and Wang X J 2015 *Rev. Sci. Instrum.* **86** 073702

[16] Siwick B J, Dwyer J R, Jordan R E and Miller R J D 2004 *Chem. Phys.* **299** 285

[17] Waldecker L, Bertoni R and Ernstorfer R 2015 *J. App. Phys.* **117** 044903

[18] Robinson M S, Lane P D and Wann D A 2014 *Rev. Sci. Instrum.* **86** 013109

[19] Gao M, Jean-Ruel H, Cooney R R, Stampe J, de Jong M, Harb M, Sciaini G, Moriena G and Miller R J D 2012 *Opt. Express* **20** 799

[20] Van Oudheusden T, de Jong E F, van der Geer S B, Op't Root W P E M, Luiten O J and Siwick B J 2007 *J. Appl. Phys.* **102** 093501

[21] Chatelain R P, Morrison V R, Godbout C and Siwick B J 2012 *Appl. Phys. Lett.* **101** 081901

[22] Kassier G H, Haupt K, Erasmus N, Rohwer E G and Schwoerer H 2009 *J. Appl. Phys.* **105** 113111

[23] Eichberger M, Erasmus N, Haupt K, Kassier G, von Flotow A, Demsar J and Schwoerer H 2013 *Appl. Phys. Lett.* **102** 121106

[24] Kassier G H 2010 *PhD Thesis*, Stellenbosch University

[25] Gahlmann A, Tae Park S and Zewail A H 2008 *Phys. Chem. Chem. Phys.* **10** 2894

[26] Williamson J C and Zewail A H 1991 *P. Natl. Acad. Sci. USA* **88** 5021

[27] Ihee H, Lobastov V A, Gomez U M, Goodson B M, Srinivasan R, Ruan C Y and Zewail A H 2001 *Science* **291** 458

[28] Rose T S, Rosker M J and Zewail A H 1988 *J. Chem. Phys.* **88** 6672

[29] Williamson J C and Zewail A H 1993 *Chem. Phys. Lett.* **209** 10

[30] Siwick B J, Dwyer J R, Jordan R E and Miller R J D 2002 *J. Appl. Phys.* **92** 1643

[31] Rangarajan L M and Bhide G K 1980 *Vacuum* **30** 515

[32] Hargittai I and Hargittai M, Stereochemical Applications of Gas-Phase Electron Diffraction – Part A, VCH Verlag, Weinheim, Germany, 1988.

[33] Sciaini G and Miller R J D 2011 *Rep. Prog. Phys.* **74** 096101

[34] Baum P 2013 *Chem. Phys.* **423** 55

[35] McCulloch A J, Sheludko D V, Saliba S D, Bell S C, Junker M, Nugent K A and Scholten R E 2011 *Nat. Phys.* **7** 785

[36] Bainbridge A R and Bryan W A 2014 *New J. Phys.* **16** 103031

[37] Kirchner F O, Lahme S, Krausz F and Baum P 2013 *New J. Phys.* **15** 063021.

[38] Portman J, Zhang H, Tao Z, Makino K, Berz M, Duxbury P M and Ruan C-Y 2013 *Appl. Phys. Lett.* **103** 253115

[39] Tao Z, Zhang H, Duxbury P M, Berz M and Ruan C-Y 2012 *J. Appl. Phys.* **111** 044316

[40] van der Geer S B, Luiten O J, de Loos M J, Pöplau G and van Rienen U 2005 *Institute of Physics Conference Series* **175** 101.

[41] Pöplau G, van Rienen U, van der Geer B and de Loos M 2004 *IEEE T. Magn.* **40** 714

[42] Siwick B J 2004 *PhD Thesis*, University of Toronto

[43] Baum P and Zewail A H 2006 *P. Natl. Acad. Sci. USA* **103** 16105